



# Reviews and syntheses: Flying the satellite into your model: on the role of observation operators in constraining models of the Earth system and the carbon cycle

Thomas Kaminski<sup>1</sup> and Pierre-Philippe Mathieu<sup>2</sup>

<sup>1</sup>The Inversion Lab, Tewssteg 4, 20249 Hamburg, Germany

<sup>2</sup>European Space Agency ESRIN, Via Galileo Galilei, Casella Postale 64, 00044 Frascati (Rome), Italy

Correspondence to: Thomas Kaminski (thomas.kaminski@inversion-lab.com)

Received: 2 June 2016 – Discussion started: 8 June 2016

Revised: 13 January 2017 – Accepted: 13 January 2017 – Published: 8 May 2017

**Abstract.** The vehicles that fly the satellite into a model of the Earth system are *observation operators*. They provide the link between the quantities simulated by the model and the quantities observed from space, either directly (spectral radiance) or indirectly estimated through a retrieval scheme (biogeophysical variables). By doing so, observation operators enable modellers to properly compare, evaluate, and constrain their models with the model analogue of the satellite observations. This paper provides the formalism and a few examples of how observation operators can be used in combination with data assimilation techniques to better ingest satellite products in a manner consistent with the dynamics of the Earth system expressed by models. It describes commonalities and potential synergies between assimilation and classical retrievals. This paper explains how the combination of observation operators and their derivatives (linearizations) form powerful research tools. It introduces a technique called automatic differentiation that greatly simplifies both the development and the maintenance of code for the evaluation of derivatives. Throughout this paper, a special focus lies on applications to the carbon cycle.

analyses of relevant processes, and their interaction and feedback mechanisms). ESM applications range from numerical weather prediction (NWP), to seasonal or decadal forecasting (see e.g. Stockdale et al., 2011; Smith et al., 2013), to climate projections on centennial scales (IPCC, 2014) or even longer (Jungclaus et al., 2010).

Before being used for predictions, ESMs and their components should be confronted with observations in order to assure their realism (validation). Such validation procedures can be extended to standardized assessments of model performance in so-called benchmarking systems by evaluation of a set of observation-based metrics (see e.g. Blyth et al., 2011; Luo et al., 2012). This involves the definition of metrics that quantify the model performance through the fit to observations. A further step towards the rigorous use of the observations is their ingestion in formal data assimilation procedures, e.g. to constrain the model's initial state (initialization) or tunable parameters in the model's process representations (calibration).

Such confrontation with observations is hampered by the fact that observed and modelled quantities typically differ in nature or scale (in space and time). For example, a flask sample of the atmospheric carbon dioxide concentration provides a value at a specific point in space and time, whereas an atmospheric tracer model operates in a discretized representation of space and time, i.e. on values that refer to a box in the atmosphere and a particular period of time. Any comparison of the two quantities (modelled and observed) must hence take the uncertainty arising from this representation error into account (see e.g. Heimann and Kaminski,

## 1 Introduction

Earth system models (ESMs) are complex software that capture our knowledge of how the ocean, atmosphere, land, and ice operate and interact. ESMs provide scientists with powerful tools to better understand our global environment, its evolution, and the potential impact of human activities (e.g.

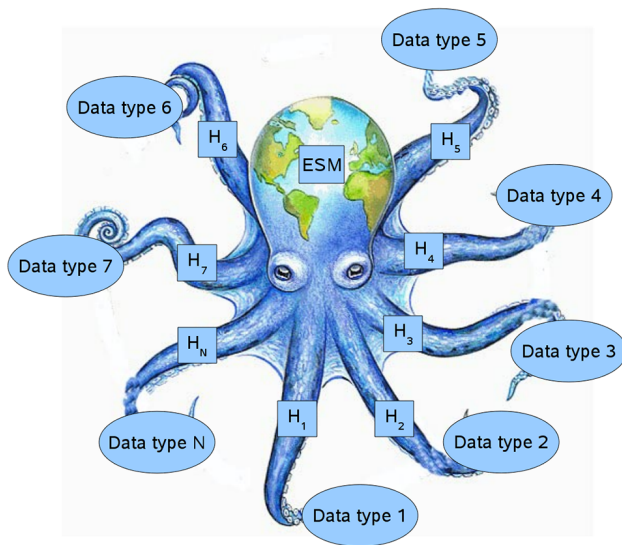


**Figure 1.** Schematic of an ESM assessing several data types via observation operators  $H_1, \dots, H_n$ .

1999). Another example is a vertical profile of the ocean temperature and salinity provided by a floating buoy (see <http://www.argo.ucsd.edu>). Again the spatial scales of the observation and the model do not match (in the horizontal dimension). In addition, ocean models are formulated in terms of potential temperature rather than temperature. Since we can only compare quantities of the same nature, some form of transformation is required before any comparison can take place. Such a difference in nature is intrinsic to observations from space, where the raw quantities measured by satellites, i.e. photon counts (Mathieu and O'Neill, 2008), are by nature only indirectly (through radiative transfer processes) related to the model quantities of interest.

The link from the model to the observations is provided through a set of relationships expressed in terms of an observation operator. We can think of an observation operator as an arm that enables the ESM to access a particular type of observation (see Fig. 1). We stress that the usage of the term operator is not meant to imply the linearity of the observation operator. In fact, observation operators range in complexity from a simple interpolation or integral scheme up to a chain of sophisticated non-linear radiative transfer models.

The layout of the remainder of this paper is as follows. Section 2 introduces the concept of an observation operator and presents examples. The role of observation operators in applications is presented in Sect. 3. Section 4 highlights the use of derivatives of observation operators and introduces *automatic differentiation*, a technique to provide these derivatives. Finally, Sect. 5 draws conclusions.

## 2 Observation operators

### 2.1 Definition

Mathematically, the observation operator is defined as mapping  $H$  from the vector of state variables  $z$  (of the model) onto the vector of observations  $y$ :

$$H : z \mapsto y. \quad (1)$$

The observation vector can include, for example, observed radiances, radar backscatter, or in situ observations. The vector of the model's state variables (*state vector*) defines the simulated system for a given time step at all points in space, and the evolution of the system is described by a sequence of state vectors forming a trajectory through the state space. We note that Eq. (1) may be generalized in the sense that the simulation of observations of temporal averages or integrals (e.g. an increment in above-ground biomass over several years or an albedo covering several weeks) may require not only a single state, but also the trajectory over the averaging/integration interval. The state variables of a dynamical model are also called prognostic variables, to contrast them with diagnostic variables, which are computed from the state and evolve only indirectly through the evolution of the state. For example, the albedo of the land surface is diagnosed from the state of the vegetation–soil system. Hence, if we achieve a change in the model state at any given point in time, the model will then propagate this change of state forward in time, and we achieve a change of the model trajectory (e.g. to improve the fit to observations). This means that to bring observational information into the model, we must link the observations to the state; in other words, the model's state vector constitutes the interface between the model and the observation operator.

The solid path in Fig. 2 sketches how an observation operator ( $H_1$ ) enables the comparison of simulated and observed values at the sensor level, i.e. at the level of spectral radiances, typically referred to as level 1 data products (Arvidsson et al., 1986). Another way to make Earth observation (EO) data accessible to dynamical models is by deriving, by means of a retrieval algorithm, a biogeophysical variable (in the following denoted as a geophysical variable) from the satellite observations. Such EO products are usually called level 2 data products (and level 3 refers to products on a space–time grid). Internally, the retrieval algorithm also relies on a functional relationship that maps the geophysical variable(s) of interest onto the spectral radiance. This mapping is similar, if not identical to, the observation operator  $H_1$ , although the term used by the EO community is *forward model*. The retrieval can be regarded as an inversion of  $H_1$ . As the examples below will illustrate, the retrieved level 2 product will typically not exactly coincide with a component of the model state vector. Hence, the confrontation of level 2 data with the model (the dotted path in Fig. 2) also requires an observation operator (denoted by  $H_2$ ).

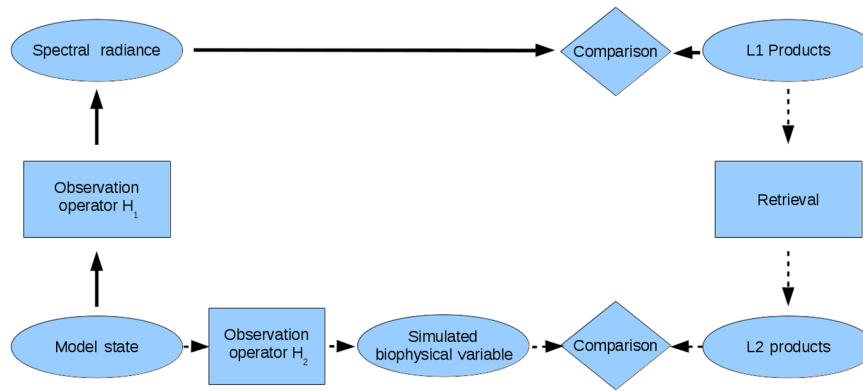


**Figure 2.** Model–data comparison at the sensor level (level 1, solid arrows) and at the level of geophysical variables (level 2, dotted arrows). Ovals denote data, and rectangles denote some form of processing.

## 2.2 Examples

Figure 3 attempts to sketch a generic observation operator  $H_1$ , which links a model’s state vector to observed spectral radiance. For the sake of clarity, the figure focuses on processing steps that map one variable onto another and omits further important steps that involve transformations in space and time, i.e. interpolation, averaging, or orbit simulation.

The simulation of spectral radiances at the sensor level requires information from the atmosphere and the land/ocean surface, including the description of ice or snow covers. Hence, the observation operator typically consists of various modules. First, from the model state, the relevant electromagnetic signatures are simulated. For example, for a passive optical sensor observing the terrestrial vegetation, this would be the reflected sunlight, and it would be computed by a model of the radiative transfer within the canopy; for examples, see Pinty et al. (2006) or Loew et al. (2014). For a passive microwave sensor that observes sea ice and snow, this would be the thermal emission, and it would involve a model of the radiative transfer within the sea ice and snowpack (see e.g. Wiesmann and Mätzler, 1999; Tonboe et al., 2006). In the atmosphere, this could be a model for the emissivity of clouds as a function of the atmospheric state. The next step covers the path through the atmosphere from the observed components to the sensor and requires a model of the radiative transfer through the atmosphere. Prime examples are the Radiative Transfer for the TIROS Operational Vertical Sounder (RTTOV; Eyre, 1991; Saunders et al., 1999) for the microwave and infrared domain, the Second Simulation of a Satellite Signal in the Solar Spectrum, 6S (Vermote et al., 1997), for the solar domain, or the optimal spectral sampling (OSS) method (Moncet et al., 2008). The output of the radiative transfer model can be compared with a level 1 product.

Each type of observation requires its own observation operator in order to be accessible to a model. The complexity of the observation operator typically reflects a compromise be-

tween the accuracy required for the application at hand and the available computational resources. In a space mission, the observation operator depends on characteristics such as the geometry of the observation (as a function of the orbit of the platform) or the measuring principle and therefore the spectral sensitivity of the sensor. The observation operator also depends on the formulation of the dynamical model. One aspect is the state space, which depends on the model formulation. For example, an atmospheric model can either diagnose clouds or include them in the state space (Chevallier et al., 2004). In the former case, the diagnostic cloud model is part of the observation operator; in the latter, it is not. Even though parts of an observation operator are usually model-dependent, it is desirable to implement the observation operator in a modular form with carefully designed interfaces. This modularity maximizes the flexible use and reuse for assimilation and retrievals and the adaptation to new models or observations; i.e. it ensures multifunctionality.

The crucial role of observation operators is reflected in comparison exercises, such as the radiation transfer model intercomparison (RAMI) initiative for the transfer of radiation in plant canopies and over soil surfaces (Pinty et al., 2001; Widlowski et al., 2007, 2013, 2015). A similar activity for the atmosphere is the international project Intercomparison of 3-D Radiation Codes (I3RC) (Cahalan et al., 2005). The I3RC focuses on the interaction of solar and thermal radiation with cloudy atmospheres. Another activity in this domain is the Cloud Feedback Model Intercomparison Project (CFMIP), which has set up the CFMIP Observation Simulator Package (COSP) (Bodas-Salcedo, 2011). The modular package includes a set of observation operators that map model output consisting of “vertical profiles of temperature, humidity, hydrometeor (clouds and precipitation) mixing ratios, cloud optical thickness and emissivity, along with surface temperature and emissivity” onto a set of level 2 products retrieved from “the following instruments: CloudSat radar, CALIPSO lidar, ISCCP, the MISR, and the Moderate Resolution Imaging Spectroradiometer (MODIS)”

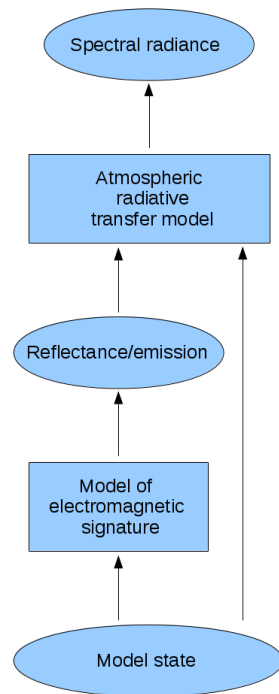


**Figure 3.** Generic scheme of an observation operator for spectral radiance. Oval boxes denote data, and rectangular boxes denote processing.

(Bodas-Salcedo, 2011). The above-mentioned “fast radiative transfer code RTTOV can also be linked to COSP to produce clear-sky brightness temperatures for many different channels of past and current infrared and passive microwave radiometers” (Bodas-Salcedo, 2011). Not only does COSP greatly simplify the comparison of model output with EO products, but using standardized interfaces also allows the comparison of multiple models through the same observation operators with EO data from various sources; this facilitates the attribution of a model–data mismatch to aspects of the model, the observation operator, or the observations. The Community Microwave Emission Modelling Platform (CMEM; Drusch et al., 2009) takes a similar role for the modelling of the emissivity of the canopy–soil system in the spectral domain from 1 to 20 GHz. For example, de Rosnay et al. (2009) use 12 different configurations of the modular system in their Land Surface Models Intercomparison Project (ALMIP).

### 3 Applications of observation operators

This section starts with an introduction of the formalism behind advanced data assimilation and retrieval schemes. The details of the formalism are useful to understand the application examples in this section (and the commonalities between assimilation and retrievals) and the need for derivative information that is discussed in Sect. 4.

#### 3.1 Formalism of data assimilation and retrieval

Data assimilation is a procedure to combine the information from observations with the information in a dynamical model. There is a range of data assimilation techniques with varying degrees of sophistication. The simplest techniques try to replace a component of the model state vector with an observation or, more precisely, some average of the two. More advanced approaches can assimilate observations  $y$  that are linked to the state through an observation operator  $H$ , which can be an observation operator for in situ data or for EO data; for example, the operators  $H_1$  and  $H_2$  introduced in Sect. 2 (see Eq. 1 and Fig. 3). The assimilation problem is typically formalized as a minimization problem for a misfit function

$$J(\mathbf{x}) = \frac{1}{2}(\mathbf{H}(\mathbf{x}) - \mathbf{y})^T \mathbf{U}_y^{-1} (\mathbf{H}(\mathbf{x}) - \mathbf{y}) + \frac{1}{2}(\mathbf{x} - \mathbf{x}_{\text{pr}})^T \mathbf{C}_{\text{xpr}}^{-1} (\mathbf{x} - \mathbf{x}_{\text{pr}}) , \quad (2)$$

where  $\mathbf{x}$  denotes the vector of unknowns. Even though in some applications this vector of unknowns may coincide with the model state,  $\mathbf{z}$ , this is not generally the case (as will be discussed below), and we need to make a clear distinction between the both objects.

The function  $J(\mathbf{x})$  is composed of two terms. The first term quantifies the misfit between the observations and their simulated counterpart (observational term).  $\mathbf{U}_y$  has to account for the uncertainty in the observations and the uncertainty imposed by the imperfection of the model, including the above-mentioned representativeness in space and time. For diagonal  $\mathbf{U}_y$  (uncorrelated uncertainty), it reduces to a least squares fit to observations. The second term quantifies the deviation of the model state from the prior information  $\mathbf{x}_{\text{pr}}$  (prior term, also called background). This term provides a means to include information in addition to the observational information into the assimilation procedure, and it ensures the existence of a minimum in cases where the observational information is not sufficient to constrain the unknowns. Both terms, observation misfit and prior, are weighted in inverse proportion to the respective uncertainties, i.e. the combined uncertainty in the observations and observation operator,  $\mathbf{U}_y$ , and the uncertainty in the prior information,  $\mathbf{U}_{\text{xpr}}$ . The superscript T denotes transposition. Note that the equation does not require the observations to be provided on the space–time grid of the model. The observations can come in any spatio-temporal distribution, e.g. the above-mentioned point measurements or orbits, as long as we can formulate the appropriate observation operator.

Equation (2) formalizes what in numerical weather prediction is called three-dimensional variational assimilation (3D-Var; Courtier et al., 1998); more precisely, it formalizes its analysis step, which is then followed by a forecast step. Operationally, the assimilation scheme is run in cyclic mode through these two steps. In such a cyclic scheme, the prior in-

formation is provided by the previous forecast; i.e. it is consistent with the dynamical information from the model, and at the same time it suffers from the errors in the model. In this setup, the specification of the prior uncertainty is particularly challenging (see e.g. Bannister, 2008a, b).

The model dynamics are even more emphasized when the scheme of Eq. (2) is extended to contain observations  $y_i$  at different time steps ( $i = 1, \dots, n$ ) to constrain the initial state  $z_0 = x$  through

$$J(\mathbf{x}) = \frac{1}{2} \sum_{i=1,n} (H(z_i(\mathbf{x})) - y_i)^T \mathbf{U}_{y_i}^{-1} (H(z_i(\mathbf{x})) - y_i) + \frac{1}{2} (\mathbf{x} - \mathbf{x}_{pr})^T \mathbf{U}_{xpr}^{-1} (\mathbf{x} - \mathbf{x}_{pr}). \quad (3)$$

This is the setup of the analysis step in four-dimensional variational assimilation (4D-Var) schemes, where the dynamical model  $M$  is used as a constraint that links the states at all observation times via

$$z_{i+1} = M(z_i) \quad (4)$$

to the initial state  $z_0 = x$ . For convenience, the notation suppresses the time-dependent nature of  $H$  and  $M$ , and it also assumes that the data uncertainties at different time steps are uncorrelated. While 4D-Var solves a single minimization problem to find a (dynamically consistent) model trajectory, 3D-Var is a sequential approach, i.e. it solves a sequence of minimization problems, which that yield a dynamically inconsistent sequence of model states. In operational NWP, as mentioned above, the application of 4D-Var is in a cyclic procedure, i.e. also in a sequential manner. Section 3.2 will describe applications where this is not the case.

In the 4D-Var approach, the vector of unknowns  $\mathbf{x}$  can be extended from the initial state to boundary values and process parameters (model calibration). Since these are external controls to the dynamical system,  $\mathbf{x}$  is also called control vector, a term taken from control theory (Lions, 1971). We usually try to select the control vector such that it comprises the fundamental unknowns of the system at hand, i.e. those with the highest uncertainty (Kaminski et al., 2012b). An extension of the 4D-Var approach (weak constraint 4D-Var) allows deviations from the model trajectory, which are included as additional components into the control vector (see e.g. Zupanski, 1997).

The *Kalman filter* is another sequential approach. Its analysis step solves a slightly simplified form of Eq. (2), in which  $H$  is replaced by its linearization  $\mathbf{H}$  (Jacobian matrix) around the prior. This allows an analytic solution  $\mathbf{x}_{po}$  of Eq. (2)

$$\mathbf{x}_{po} = \mathbf{x}_{pr} - \mathbf{U}_{xpo} \mathbf{H}^T \mathbf{U}_y^{-1} (\mathbf{H} \mathbf{x}_{pr} - y_i), \quad (5)$$

the evaluation of which involves the inversion of the matrix

$$\mathbf{U}_{xpo} = (\mathbf{H}^T \mathbf{U}_y^{-1} \mathbf{H} + \mathbf{U}_{xpr}^{-1})^{-1}, \quad (6)$$

which is typically of high dimension (e.g.  $10^7$  in NWP) and expresses the uncertainty range in  $\mathbf{x}_{po}$  that is consistent with uncertainty ranges in the data and the prior values.

In the case of linear  $H$  and Gaussian probability densities for the prior and the data, the solution of Eq. (2) is Gaussian as well and therefore completely described by its mean (Eq. 5) and covariance (Eq. 6). This formalism is, for example, applied in inverse modelling of the atmospheric transport of carbon dioxide (Enting, 2002), where an atmospheric transport model takes the role of  $H$  and the space–time distribution of the surface fluxes takes the role of  $\mathbf{x}$ . Note that the cost function’s second derivative (Hessian matrix)  $\mathbf{J}''$  is related to  $\mathbf{U}_{xpo}$  through

$$\mathbf{U}_{xpo} = \mathbf{J}''(\mathbf{x})^{-1}. \quad (7)$$

In the non-linear case (i.e.  $H$  or  $M$  are non-linear), we cannot solve Eq. (2) or Eq. (3) analytically, but via the cost function’s Hessian we can use Eq. (7) to approximate  $\mathbf{U}_{xpo}$ . Via a linearization  $\mathbf{N}$  of the model that links the control variables to model outputs of interest  $f$ , we can approximate the uncertainty range of these model outputs  $\mathbf{U}_f$  by

$$\mathbf{U}_f = \mathbf{N} \mathbf{U}_{xpo} \mathbf{N}^T. \quad (8)$$

The alternative to the above assimilation approaches (which are based on linearizations) are ensemble methods, such as Markov chain Monte Carlo (see e.g. Metropolis et al., 1953), ensemble Kalman filter (Evensen, 2003) techniques, or particle filters (see e.g. van Leeuwen, 2009), which rely on forward simulations to sample the control space. The feasible ensemble size is limited by the computational demands, which are essentially determined by the complexity of the underlying model. We also note the challenge of filter degeneracy that limits the applicability of particle filters to high-dimensional problems (see e.g. Snyder et al., 2008).

We used Eq. (2) to introduce the formalism of data assimilation. The same equation also plays a central role in retrievals. The minimization of Eq. (2) describes a retrieval algorithm for the entire state. The prior term regularizes what is otherwise an underdetermined inverse problem: several of the unknown variables that influence the observed signal vary continuously with altitude (continuous vertical profiles). Even though we formulate our observation operators on a vertical grid, there are typically “fewer” measurements than unknowns. Consequently, there are many sets of unknown variables that yield an equal fit to observations; i.e. we have to deal with a non-zero null space (Tarantola, 2005). The word fewer was put in quotation marks to indicate that, more precisely, it is not only the ratio of the numbers of observations to unknowns that matters here, but it is also the capability of the observations to constrain the unknowns. The null space is the subspace of the control space that is not constrained by the observations, and including more observations of the same type often does not help to reduce the

dimension of the null space. The prior term provides additional information on every unknown and helps the retrieval algorithm to find a unique solution. Further, Eqs. (6) or (7) are used to furnish the retrievals with uncertainty ranges.

Another perspective on the assimilation of level 1 data is to regard it as an advanced form of retrieval, and to regard the assimilation system as an advanced retrieval algorithm that optimally combines the information from remote sensing, radiative transfer, and dynamical model. The other point to note is that  $H$  is usually not constant in space and time. For example, the radiative transfer in the optical domain is affected by atmospheric water vapour and aerosols. A retrieval of a land surface variable, for example, requires information on clouds and aerosols. In a coupled atmosphere–land model, these data are available in a form that is dynamically consistent with the state of the land surface; on the other hand, they are also affected by errors in the model.

### 3.2 Data assimilation examples

The prime example of an atmospheric 4D-Var system is the one (Rabier et al., 2000) operated at the European Centre for Medium-Range Weather Forecasts (ECMWF) in their Integrated Forecasting System (IFS; Courtier et al., 1998). The 4D-Var system has been in operation since 2003; meanwhile, most of the assimilated observations are remotely sensed radiances. Observations are provided by about 50 different sensors and used with appropriate observation operators. The system is used with a 12 h assimilation window to initialize the operational forecast. Several other weather services (including those of Canada, France, and the UK) are running similar 4D-Var systems. A recent development at NWP centres are hybrid approaches that combine ensemble and variational approaches. Such a hybrid approach is operational at ECMWF (Buizza et al., 2008; Isaksen et al., 2010; Bonavita et al., 2012) and the NWP centres of the UK (Clayton et al., 2013) and Canada (Buehner et al., 2010).

A prominent example of a variational ocean assimilation system was set up around the MIT General Circulation Model (MITgcm; Marshall et al., 1997) by the consortium ECCO: Estimating the Circulation and Climate of the Ocean (see <http://www.ecco-group.org>). The system (Stammer et al., 2002) uses a combination of in situ observations and level 2 or 3 remote-sensing products (including sea surface height, sea surface temperature, wind stress, and geoid) for ocean state estimation over decadal-scale assimilation windows (Wunsch and Heimbach, 2006). Owing to these long assimilation windows, the prescribed exchange fluxes with the atmosphere are a major source of uncertainty in their model trajectory. Hence, this boundary condition is included in the control vector along with the initial state. Various applications of the assimilation product require closed property budgets over the entire assimilation window, which are achieved via variational approaches in contrast to sequential approaches. Examples are mechanistic and diagnostic stud-

ies of climate variability or oceanic tracer transport problems (Wunsch et al., 2009).

A recent example of a regional variational assimilation system for the coupled ocean–sea-ice system in the northern latitudes was developed by Kauker et al. (2015). This system is operated for assimilation windows from a few weeks to a few years. Their control vector combines (depending on the application) the initial state, boundary conditions, and process parameters. The system is constrained by hydrographic in situ observations and level 2 and 3 products of sea surface temperature, sea ice concentration, thickness, and displacement.

An example of the global terrestrial vegetation is provided by the Carbon Cycle Data Assimilation System (CCDAS). Initially set up for the assimilation of in situ observations of the atmospheric CO<sub>2</sub> concentration (Rayner et al., 2005), the system was extended step by step with observation operators for several level 2 or 3 products, namely fraction of absorbed photosynthetically active radiation (FAPAR) products (Knorr et al., 2010; Kaminski et al., 2012a), the column-integrated atmospheric carbon dioxide concentration (XCO<sub>2</sub>) (Kaminski et al., 2010, 2016b), and the surface layer soil moisture (Scholze et al., 2016). The observation operator for FAPAR was a considerable extension of the previous system because it required modules for the simulation of vegetation phenology and hydrology, which were previously provided by an offline calculation. The observation operators for CO<sub>2</sub> and XCO<sub>2</sub> include models of the atmospheric transport that solve the continuity equation for carbon dioxide (Heimann, 1995; Heimann and Körner, 2003). The observation operator for surface layer soil moisture was derived by modification of the initial bucket formulation of the soil hydrology model (which had no equivalent to the thin surface layer that is observed from space). The assimilation window ranges from years to decades. Considering uncertain values of the parameters (constants) in process formulations as the major source of uncertainty in the model trajectory, the control vector is composed of (depending on the setup) 50–100 (in extreme cases up to 1000) process parameter values. This type of application is called parameter estimation or model calibration.

### 3.3 Retrieval examples

The integrated retrieval of Toudal (1994) or Melsheimer et al. (2009) solves simultaneously for geophysical variables (level 2 data) of the atmosphere (wind speed, total water vapour, cloud liquid water), the ocean (sea surface temperature), and the sea ice (ice surface temperature, total sea ice concentration, multi-year ice fraction). Technically, as  $H$  is non-linear, Toudal (1994) and Melsheimer et al. (2009) use Eq. (5) in an iterative procedure ( $\mathbf{x}_{po}$  from one step is provided as  $\mathbf{x}_{pr}$  to the subsequent step), which recomputes  $\mathbf{H}$  by linearization around the current  $\mathbf{x}_{pr}$ . Upon convergence, they deliver posterior uncertainties via Eq. (6). Their input values are radiances (brightness temperatures) observed by the Ad-

vanced Microwave Scanning Radiometer for EOS (AMSR-E). Their prior values are taken from a range of sources, including analysis data provided by an NWP assimilation system, or separate univariate retrievals. This integrated retrieval is performed individually for each observed point in space and time at 12.5 km horizontal resolution. Although the use of the same level 1 data in an assimilation system (ensuring dynamical consistency between the atmosphere, ocean, and sea ice components) appears desirable, it is highly challenging in various respects: from a software development perspective, because it would require an assimilation system built around a coupled atmosphere, ocean, and sea ice model; from a computational perspective, because a single run of the coupled model at 12.5 km resolution is already computationally expensive, and an iterative assimilation scheme would be more so.

An example of the land surface is the Joint Research Centre Two-stream Inversion Package (JRC-TIP) (Pinty et al., 2007), which solves Eq. (2) for model parameters controlling the radiation transfer regime in vegetation canopies, namely the effective leaf area index (LAI) and the spectral scattering properties of the vegetation and the soil. The latter information is then used to compute the spectral fluxes scattered by, absorbed in, and transmitted through the vegetation layer as well the fluxes absorbed in the background (radiant fluxes). Further, the system uses Eq. (7) to infer the uncertainty in the retrieved parameters and Eq. (8) to propagate these forward to uncertainties in the simulated radiant fluxes. In its typical setup, the system uses observed albedos in two broad wavebands (visible and near infrared) (Pinty et al., 2007, 2011a, b). The JRC-TIP is constructed around a one-dimensional two-stream model, which takes three-dimensional radiative transport effects into account (Pinty et al., 2006). As a consequence, the retrieved vegetation parameters are effective parameters (i.e. their values are only meaningful within this model) and are determined such that the radiant fluxes are simulated as accurately as possible. This illustrates a crucial point when confronting retrieved level 2 variables with their ESM counterparts. It is essential that the variables have the same definition in the forward model that is used for the retrieval and in the observation operator that is used for its assimilation. For the JRC-TIP products, this is the case for the radiant fluxes and soil parameters; for the effective vegetation parameters, it requires the use of the same two-stream model in the observation operator. An in-depth description of JRC-TIP, its use for the generation of EO products, and the validation of these products is provided by a dedicated contribution to this special issue (Kaminski et al., 2016a).

The Earth Observation Land Data Assimilation System (EO-LDAS, Lewis et al., 2012) is a retrieval and data assimilation framework for various types of EO data. Primarily, it uses a weak-constraint variational approach, i.e. the weak constraint form of Eq. (3), in combination with a simple model of the land surface dynamics (e.g. persistence), which acts as a regularization in the spatial and temporal domains.

The system can, however, also perform single-pixel retrievals or be operated in a sequential manner. EO-LDAS development started for the optical domain with the semi-discrete model of the vegetation canopy (Gobron et al., 1997) as observation operator. The system is being extended with further observation operators, including the above-mentioned CMEM for passive microwave observations. This means it has the capability to simultaneously use EO over a range of spectral domains and exploit their complementarity. To achieve the computational performance necessary for global-scale processing of high-resolution EO data, the system is also operated (Gómez-Dans et al., 2016) with fast approximations of radiative transfer (RT) models (including the above-mentioned atmospheric RT code 6S) by so-called emulators. A similar regularization strategy in the temporal domain was also presented by Lauvernet et al. (2008), who operated a variational inversion scheme around a chain of coupled RT models, i.e. PROSPECT (Jacquemoud and Baret, 1990) for the leaf optical properties, Scattering by Arbitrarily Inclined Leaves, SAIL (Verhoef, 1984), for the canopy RT, and the Simplified Method for Atmospheric Correction, SMAC (Rahman and Dedieu, 1994), for the atmospheric RT.

A serious practical difficulty in data assimilation is the specification of  $\mathbf{U}_y$ . This is particularly relevant in multi-data stream assimilation because  $\mathbf{U}_y$  defines the respective weights of the data streams. In the case of level 2 data,  $\mathbf{U}_y$  is the posterior uncertainty of the retrieval. Since the retrieval is typically carried out point by point, uncertainty correlations in space and time are difficult to assess. Another issue is the data volume required by the uncertainty information. For a product of a retrieved geophysical variable at  $n$  points in space and time,  $\mathbf{U}_y$  contains (taking its symmetry into account)  $n \cdot (n + 1)/2$  different values, a volume that is usually prohibitive in real-world applications. The challenge is to develop ways of providing (approximations of)  $\mathbf{U}_y$  that retain the essential information in a minimal data volume. One approach is through appropriate variable transformations based on a singular value decomposition of the observation operator (Joiner and Da Silva, 1998; Migliorini, 2012). Another approach is a parametric model of  $\mathbf{U}_y$ , for example, as provided by Reuter et al. (2016) for the XCO<sub>2</sub> product retrieved from Scanning Imaging Absorption Spectrometer for Atmospheric CHartography (SCIAMACHY) observations through their Bremen Optimal Estimation DOAS (BESD; Reuter et al., 2011) algorithm. Generally, the contribution by the observational uncertainty  $\mathbf{U}_y$  is certainly easier to specify in the case of level 1 data. Their direct assimilation automatically propagates, through the observation operator  $H_1$ , the full information content of  $\mathbf{U}_y$  into the model.

A related topic is the consistency of the prior information ( $\mathbf{x}_{pr}$  and  $\mathbf{U}_{xpr}$  in Eq. 2) used in the retrieval scheme with the scheme that subsequently uses these retrievals in a dynamical model, e.g. for assimilation. Rodgers and Connor (2003) demonstrate how the  $\mathbf{x}_{pr}$  used in the retrieval can be replaced with that simulated by the dynamical model, provided

that the following are available:  $\mathbf{x}_{\text{pr}}$  and the so-called resolution operator (Backus and Gilbert, 1968)  $\mathbf{U}_{\text{xpo}} \mathbf{H}^T \mathbf{U}_y^{-1} \mathbf{H}$  of the retrieval (also called the averaging kernel), i.e. Eq. (5). Chevallier (2015) goes one step further and addresses the remaining inconsistencies in  $\mathbf{U}_{\text{xpr}}$  and highlights their effect in his atmospheric transport inversion using retrievals of XCO<sub>2</sub>. More generally, Migliorini (2012) derives requirements on the retrieval such that the assimilation of the retrieved level 2 products is equivalent to the direct assimilation of level 1 products.

### 3.4 Observing system simulation experiments and quantitative network design

Observing system simulation experiments (OSSEs) and quantitative network design (QND) are two methodologies that evaluate observation impact on assimilation systems. Through an observing system or observational network, we understand the superset of all observations that are made available to an assimilation system. We only give a brief introduction to the topic, as QND for the carbon cycle is addressed by another contribution to this special issue (Kaminski and Rayner, 2017).

An OSSE (see e.g. Böttger et al., 2004; Masutani et al., 2010; Timmermans et al., 2015) uses a model plus observation operators to simulate (in a model) analogues of observations that would be collected by a potential observing system (often the current observing system extended by a potential new data stream). The model is also used to simulate, in a so-called “nature run”, a surrogate of reality, i.e. a reference trajectory over the period of investigation. Then an assimilation–forecast system (preferably built around a different model) is used to evaluate some measure of the performance of the potential observing system and its subsystems. In NWP, the performance of an observing system is usually quantified by the quality (skill) of a forecast from the initial value that was constrained by the observation system. Via this procedure one can, for example, assess the added value of a planned mission in terms of an increment in forecast skill. We also note a related approach, observing system experiments (OSEs), which assess observation impact by removing one or several existing data streams from the list of observations used in a data assimilation system.

QND (for overviews, see Kaminski and Rayner, 2008, 2017) relies on the ability of an assimilation system to evaluate posterior uncertainties on target quantities of interest via Eqs. (7) and (8). For a linear model, this propagation of uncertainty is independent of the observational value; it only depends (via Eqs. 7 and 3) on the data and prior uncertainties, the sensitivity of the observations with respect to the control variables, and (via Eq. 8) the sensitivity of the target quantity  $f$  to the control variables. A first application to mission design was presented by Rayner and O’Brien (2001), who ran an atmospheric transport inversion system built around a linear model of the atmospheric transport of

carbon dioxide in QND mode. They assessed the utility of remotely sensed carbon dioxide in constraining its CO<sub>2</sub> fluxes. Their benchmark was the in situ flask sampling network. Kaminski et al. (2010) generalized the method to the above-mentioned CCDAS and assessed the utility of XCO<sub>2</sub> observations with an active lidar instrument. The performance of the observing system is quantified by posterior uncertainty of surface fluxes and compared to the performance of the in situ network. Kaminski et al. (2012a) use CCDAS to assess the performance of potential optical sensor configurations in constraining the vegetation’s carbon and water fluxes. Their benchmark was the Medium Resolution Imaging Spectrometer (MERIS) sensor. Another QND application (Kaminski et al., 2015) evaluated airborne sampling strategies for sea ice thickness and snow depth in the Arctic using simultaneous laser altimeter and snow radar observations.

For both approaches, OSSE and QND, the importance of suitable observation operators is obvious. A disadvantage is that the result depends on the model. Both techniques require the specification of data uncertainties for the hypothetical data streams to be evaluated.

## 4 Derivatives of observation operators

This section first summarizes how the capability to evaluate derivatives of the observation operator is used in efficient schemes for retrieval, assimilation, or QND. It then introduces a technique for providing derivative information.

In variational assimilation, Eqs. (2) or (3) are typically minimized in an iterative procedure that varies  $\mathbf{x}$ . To do this efficiently, even for high-dimensional control spaces, so-called gradient algorithms are employed. They rely on the capability of evaluating the gradient of  $J$  with respect to  $\mathbf{x}$  to define a search direction in the space of unknowns. The gradient is useful because it yields the direction of steepest ascent. For  $J(\mathbf{x})$  of Eq. (2), straightforward differentiation with respect to  $\mathbf{x}$  yields (see Sect. 3.4.4 of Tarantola, 2005) the gradient

$$\nabla J(\mathbf{x}) = \mathbf{H}(\mathbf{x})^T \mathbf{U}_y^{-1} (H(\mathbf{x}) - \mathbf{y}) + \mathbf{U}_{\text{xpr}}^{-1} (\mathbf{x} - \mathbf{x}_{\text{pr}}), \quad (9)$$

and we see that its evaluation requires the capability to multiply the transpose of  $\mathbf{H}$  with a vector. The uncertainty estimation via Eq. (7) based on  $\mathbf{J}''$  additionally requires second derivative information on  $H$ . This second derivative expresses the curvature of (the components) of  $H$ , i.e. the change of its linearization corresponding to a unit change of  $\mathbf{x}$ .

Likewise, the Kalman filter requires derivatives of  $H$ : in Eq. (5), it multiplies the matrix  $\mathbf{H}$  and its transpose with vectors, and for the evaluation of Eq. (6) it needs to invert a matrix that contains  $\mathbf{H}$  and its transpose. One can do this inversion by pre-computing  $\mathbf{H}$  or by so-called matrix-free methods that repeatedly multiply  $\mathbf{H}$  and its transpose with vectors.

As mentioned, advanced retrieval algorithms are based on the same equations; i.e. they typically solve Eq. (2) either via gradient methods or the (possibly repeated) application of Eq. (5) and use either Eq. (7) or its approximation Eq. (6) to estimate the posterior uncertainty. Hence, they benefit in the same way from derivatives of  $H$  as data assimilation systems. The same holds for QND schemes, which are based on the computation of uncertainties via Eq. (7) or its approximation, Eq. (6).

Traditionally, derivatives were approximated by multiple forward runs (finite difference approximation) (see e.g. Toudal, 1994; Melsheimer et al., 2009; Govaerts et al., 2010; Dubovik et al., 2011). This discretized procedure has two disadvantages. The first is the limited accuracy of this gradient approximation (providing only the linear term of the Taylor series), which degrades the performance of the above-listed algorithms. For example, incorrect gradient information will slow down or prematurely stop the iterative minimization of  $J$ , because gradient-based minimization algorithms rely on the consistency of evaluations of  $J$  and its gradient. The other disadvantage is that the computational cost of this approximation grows linearly with the length of the control vector.

Both disadvantages can be avoided by automatic differentiation (AD; Griewank, 1989). AD is a procedure that generates source code for the evaluation of derivatives from the code of the underlying function. In the current case, this function is the observation operator mapping the state variables onto remote-sensing products. The function code is decomposed into elementary functions (such as  $+$ ,  $-$ ,  $\sin(\cdot)$ ), for which the derivative (local Jacobian) is straightforward to derive. The derivative of the composite function is then constructed via the chain rule as the product of all local Jacobians. According to the associative law, this multiple matrix product can be evaluated in arbitrary order without changing the result. The *tangent linear* code (or tangent code) does this evaluation in the same order as the function is evaluated, which is called the *forward mode* of automatic differentiation. The *adjoint* code uses exactly the opposite order, which is called the *reverse mode* of automatic differentiation. Even though both modes yield the same derivative, depending on the dimensions of the function to be differentiated, there may be large differences in their computational efficiency. The CPU time required by the tangent code is proportional to the number of the function's input variables but independent of the number of output variables. By contrast, the CPU time required by the adjoint code is proportional to the number of output variables and independent of the number of input variables. Both the tangent and adjoint codes use values from the function evaluation (*required values*) (see e.g. Giering and Kaminski, 1998; Hascoët et al., 2004). Providing required values to the adjoint code is more complicated than to the tangent code. As an application of the chain rule, AD provides derivatives that are accurate up to rounding error.

For variational assimilation, we require the derivative of the scalar-valued cost function  $J(x)$  of Eqs. (2) and (3) with

respect to a usually high-dimensional vector  $x$ . For a state-of-the-art model, only the adjoint can provide this derivative with sufficient efficiency. A product  $\mathbf{H}v$  of  $\mathbf{H}$  with a vector  $v$  yields the directional derivative of  $\mathbf{H}$  in the direction defined by  $v$ , i.e. the derivative of the function  $H(x + tv)$  of a scalar independent variable  $t$ . Hence, this type of product is evaluated most efficiently in forward mode, i.e. by the tangent linear code of  $H$ . By contrast, a product of the form  $\mathbf{H}^T v$  is the (transpose of the) derivative of the scalar-valued function  $v^T H(x)$ , which is evaluated most efficiently in reverse mode, i.e. by the adjoint of  $H$ . The scalar forward and reverse modes required for efficient evaluation of the above Jacobian vector products are the standard forms of the derivative code. The *scalar mode* is contrasted by the *vector mode*. In forward mode, the vector mode simultaneously computes the sensitivities with respect to multiple input quantities, and in reverse mode it simultaneously computes the sensitivity of multiple output quantities. Experience shows that the vector mode is considerably more efficient than multiple runs in scalar mode (see e.g. Kaminski et al., 2003). We use the vector mode for applications that require the entire Jacobian,  $\mathbf{H}$ . Here the sensible choice between forward and reverse modes depends on the relative dimensions of state and observation spaces.

A particular advantage of AD is that it can guarantee readability and locality (Talagrand, 1991); i.e. every statement in the derivative code belongs to a particular statement in the function code. As a consequence, if the function code is modular, the same modularity is preserved in the derivative code. Another important advantage of the AD approach is that it simplifies the maintenance of the derivative code, because it can be quickly updated after any modification of the function code.

Since an AD tool operates at the code level, it is restricted to a particular programming language. For the most frequently used programming languages in Earth system science, namely Fortran and C, AD tools are, however, available. It is a considerable effort to develop and maintain an AD tool at a level robust enough for relevant scientific applications. Over the last decade, tool development has made good progress, and there is a long list of successful AD applications to component models of the Earth system. A prime example is the above-mentioned MITgcm, which is compliant with multiple AD tools (Forget et al., 2015). Typically, an initial effort is required to achieve the compliance of a model with an AD tool. From this basis, maintaining compliance for incremental updates of the model or the AD tool is less demanding. This is, on the one hand, because AD tool developers apply regression tests before each new release against a set of benchmarking codes to preserve compliance and; on the other hand, the incremental model updates typically respect the AD tool's coding requirements. Examples are limitations in the handling of pointers or memory allocation/deallocation sequences. It should also be noted that some AD tools allow the insertion of directives that support

the analysis of the model code. These directives are helpful (and sometimes necessary) to enhance the efficiency of the generated code.

In some cases, analytical formulations of the derivative can be derived and implemented with the observation operator (Moncet et al., 2008). Alternatively, the AD process can be mimicked by hand (see e.g. Rabier et al., 2000; Weaver et al., 2003; Moore et al., 2004; Kleespies et al., 2004; O'Dell et al., 2006; Barrett and Renzullo, 2009); i.e. a human transforms the function code line by line into derivative code following the same recipes (Giering and Kaminski, 1998) that are implemented in AD tools. The advantage of hand-coding derivatives is that a human can be more flexible than a software tool. On the other hand, the hand-coding approach is tedious and error prone. As a consequence, this approach requires considerable development and maintenance effort and is restricted to first derivatives. The large assimilation systems in the above list (Rabier et al., 2000; Weaver et al., 2003; Moore et al., 2004) were set up before AD tools were mature enough to handle the respective function codes.

Whether coded by hand or by an AD tool, the differentiation process typically reveals issues in the function code that are not apparent otherwise. A standard example is the square root e.g. used in the computation of the norm, the derivative of which tends to infinity as the argument tends to 0. Infinite sensitivities were typically not intended when the model code was designed, and we can regard a differentiable reformulation as model improvement. A further example is the introduction of a floor value of 0 to avoid negative values of the simulated ice-covered area. An obvious implementation of this floor value as the maximum of the simulated area and 0 produces a step in the derivative at 0. Another example (now for the implementation as a minimum) is the formulation of co-limitation in biogeochemical models, in particular for carbon fixation in the photosynthesis model of Farquhar et al. (1980). Kaminski et al. (2013) and Schürmann et al. (2016) describe the replacement of non-differentiabilities with smooth alternatives (including a lookup table) in a model of the terrestrial biosphere. The handling of similar non-differentiabilities in a crop model is described by Lauvernet et al. (2012). In this context, it is helpful that AD tools (see, for example, Pascual and Hascoët, 2008, for C and Fortran) support the provision of derivative code for external routines.

Xu (1996) discusses treatment non-differentiabilities in NWP models through convection, precipitation, or clouds, and Lorenc and Payne (2007) highlight the use of a statistical variational concept of 4D-Var at a convective scale. Blessing et al. (2014) explore the smoothing of non-differentiabilities, in particular of the atmospheric component of an Earth system model.

Typical formulations of leaf phenology rely on a number of on–off switches that yield non-differentiable behaviour and hamper the performance in a CCDAS. This problem was addressed by Knorr et al. (2010) through the design of an

alternative phenology model that is based on a probabilistic approach and takes spatial sub-grid variability into account. As a consequence, the model yields (more realistic) smooth transitions instead of on–off behaviour and performs well in CCDAS applications (Knorr et al., 2010; Kaminski et al., 2012a; Schürmann et al., 2016). Our recommendation is to consider the availability of the sensitivity information as an additional perspective on the model and its implementation. One can benefit from this sensitivity information and improve the modelling concept, as demonstrated for leaf phenology by Knorr et al. (2010), or remove errors in the implementation as described by Kaminski et al. (2003).

## 5 Conclusions

EO products can only be accessed by Earth system models via suitable observation operators. Hence, the careful design of observation operators is essential to optimally exploit the observational information. There are overlaps between observation operators used to confront dynamical models with EO data (validation, benchmarking, assimilation) and forward models used for retrievals of geophysical products. To allow the most flexible use, observation operators should be designed in modular form with carefully constructed interfaces. Several advanced retrieval algorithms and advanced assimilation techniques (Kalman filter, 3D-Var, and 4D-Var) rely on first derivatives (linearizations) of the observation operators, i.e. their tangent and adjoint versions. The assessment of uncertainties and quantitative network design additionally require second derivatives of observation operators. To maximize their application range, these derivative codes should be developed and maintained together with their underlying observation operators. This procedure is, for example, applied at the European Centre for Medium-Range Weather Forecasts. Automatic differentiation (AD) provides a means to minimize the development and maintenance effort for these derivative codes. There is an ever-increasing list of successful AD applications to large-scale Earth system science codes, including many observation operators. Meanwhile, there is a tendency among code developers to achieve and preserve compliance with an AD tool and thus enhance the functionality of their modelling system through the availability of derivative information. In the development of an AD-compliant modelling or retrieval system, the system's sustainability can be maximized by the selection of a mature AD tool that is permanently maintained by an experienced development team and extended in response to the evolution of user needs and programming languages. Close collaboration with AD tool developers has proven beneficial in the efficient setup of robust AD-compliant systems for modelling (see e.g. Rayner et al., 2005; Forget et al., 2015; Schürmann et al., 2016; Kaminski et al., 2016b) or retrieval (see e.g. Pinty et al., 2007; Lauvernet et al., 2008, 2012; Lewis et al., 2012).

*Data availability.* No data sets were used in this article.

*Competing interests.* The authors declare that they have no conflict of interest.

*Acknowledgements.* The authors would like to thank Laurent Bertino, Frédéric Chevallier, Patrick Heimbach, Christian Melsheimer, Bernard Pinty, and the anonymous reviewers for helpful comments. We acknowledge the support from the International Space Science Institute (ISSI). This publication is an outcome of the ISSI's Working Group on "Carbon Cycle Data Assimilation: How to Consistently Assimilate Multiple Data Streams". Thomas Kaminski was in part funded by the ESA GHG-CCI project.

Edited by: M. Scholze

Reviewed by: two anonymous referees

## References

- Arvidson, R., Billingsley, R., Chase, R., Chavez, P., Devirian, M., Estes, J., Hunolt, G., Klose, J., Ludwig, G., Mosher, F., and Rossow, W.: Report of the EOS Data Panel on the Data and Information System, Vol. Iia of NASA TM-87777, National Aeronautics and Space Administration, Washington, D.C., 1986.
- Backus, G. and Gilbert, F.: The Resolving Power of Gross Earth Data, *Geophys. J. Int.*, 16, 169–205, doi:10.1111/j.1365-246X.1968.tb00216.x, 1968.
- Bannister, R. N.: A review of forecast error covariance statistics in atmospheric variational data assimilation. I: Characteristics and measurements of forecast error covariances, *Q. J. Roy. Meteor. Soc.*, 134, 1951–1970, doi:10.1002/qj.339, 2008a.
- Bannister, R. N.: A review of forecast error covariance statistics in atmospheric variational data assimilation. II: Modelling the forecast error covariance statistics, *Q. J. Roy. Meteor. Soc.*, 134, 1971–1996, doi:10.1002/qj.340, 2008b.
- Barrett, D. J. and Renzullo, L. J.: On the Efficacy of Combining Thermal and Microwave Satellite Data as Observational Constraints for Root-Zone Soil Moisture Estimation, *J. Hydrometeorol.*, 10, 1109–1127, doi:10.1175/2009JHM1043.1, 2009.
- Blessing, S., Kaminski, T., Lunkeit, F., Matei, I., Giering, R., Köhl, A., Scholze, M., Herrmann, P., Fraedrich, K., and Stammer, D.: Testing variational estimation of process parameters and initial conditions of an earth system model, *Tellus A*, 66, doi:10.3402/tellusa.v66.22606, 2014.
- Blyth, E., Clark, D. B., Ellis, R., Huntingford, C., Los, S., Pryor, M., Best, M., and Sitch, S.: A comprehensive set of benchmark tests for a land surface model of simultaneous fluxes of water and carbon at both the global and seasonal scale, *Geosci. Model Dev.*, 4, 255–269, doi:10.5194/gmd-4-255-2011, 2011.
- Bodas-Salcedo, A. E. A.: COSP: satellite simulation software for model assessment, *B. Am. Meteorol. Soc.*, 92, 1023–1043, 2011.
- Bonavita, M., Isaksen, L., and Hólm, E. V.: On the use of EDA background error variances in the ECMWF 4D-Var, *Q. J. Roy. Meteor. Soc.*, 138, 1540–1559, doi:10.1002/qj.1899, 2012.
- Böttger, H., Menzel, P., and Pailleux, J. (Eds.): Proceedings of the third WMO Workshop on the Impact of Various Observing Systems on Numerical Weather Prediction, WMO, Geneva, 2004.
- Buehner, M., Houtekamer, P. L., Charette, C., Mitchell, H. L., and He, B.: Intercomparison of Variational Data Assimilation and the Ensemble Kalman Filter for Global Deterministic NWP. Part I: Description and Single-Observation Experiments, *Mon. Weather Rev.*, 138, 1550–1566, doi:10.1175/2009MWR3157.1, 2010.
- Buizza, R., Leutbecher, M., and Isaksen, L.: Potential use of an ensemble of analyses in the ECMWF Ensemble Prediction System, *Q. J. Roy. Meteor. Soc.*, 134, 2051–2066, doi:10.1002/qj.346, 2008.
- Cahalan, R. F., Oreopoulos, L., Marshak, A., Evans, K., Davis, A. B., Pincus, R., Yetzer, K. H., Mayer, B., Davies, R., Ackerman, T. P., Barker, H. W., Clothiaux, E. E., Ellingson, R. G., Garay, M. J., Kassianov, E., Kinne, S., Macke, A., O'Hirok, W., Partain, P. T., Prigarin, S. M., Rublev, A. N., Stephens, G. L., Szczap, F., Takara, E. E., Várnai, T., Wen, G., and Zhuravleva, T. B.: The 13RC—Bringing Together the Most Advanced Radiative Transfer Tools for Cloudy Atmospheres, *B. Am. Meteorol. Soc.*, 86, 1275–1293, 2005.
- Chevallier, F.: On the statistical optimality of CO<sub>2</sub> atmospheric inversions assimilating CO<sub>2</sub> column retrievals, *Atmos. Chem. Phys.*, 15, 11133–11145, doi:10.5194/acp-15-11133-2015, 2015.
- Chevallier, F., Lopez, P., Tompkins, A., Janisková, M., and Moreau, E.: The capability of 4D-Var systems to assimilate cloud-affected satellite infrared radiances, *Q. J. Roy. Meteor. Soc.*, 130, 917–932, 2004.
- Clayton, A. M., Lorenc, A. C., and Barker, D. M.: Operational implementation of a hybrid ensemble/4D-Var global data assimilation system at the Met Office, *Q. J. Roy. Meteor. Soc.*, 139, 1445–1461, doi:10.1002/qj.2054, 2013.
- Courtier, P., Andersson, E., Heckley, W., Vasiljevic, D., Hamrud, M., Hollingsworth, A., Rabier, F., Fisher, M., and Pailleux, J.: The ECMWF implementation of three-dimensional variational assimilation (3D-Var). I: Formulation, *Q. J. Roy. Meteor. Soc.*, 124, 1783–1807, 1998.
- de Rosnay, P., Drusch, M., Boone, A., Balsamo, G., Decharme, B., Harris, P., Kerr, Y., Pellarin, T., Polcher, J., and Wigneron, J.-P.: AMMA Land Surface Model Intercomparison Experiment coupled to the Community Microwave Emission Model: ALMIP-MEM, *J. Geophys. Res.-Atmos.*, 114, d05108, doi:10.1029/2008JD010724, 2009.
- Drusch, M., Holmes, T., de Rosnay, P., and Balsamo, G.: Comparing ERA-40-Based L-Band Brightness Temperatures with Skylab Observations: A Calibration/Validation Study Using the Community Microwave Emission Model, *J. Hydrometeorol.*, 10, 213–226, doi:10.1175/2008JHM964.1, 2009.
- Dubovik, O., Herman, M., Holdak, A., Lapyonok, T., Tanré, D., Deuzé, J. L., Ducos, F., Sinyuk, A., and Lopatin, A.: Statistically optimized inversion algorithm for enhanced retrieval of aerosol properties from spectral multi-angle polarimetric satellite observations, *Atmos. Meas. Tech.*, 4, 975–1018, doi:10.5194/amt-4-975-2011, 2011.
- Enting, I. G.: *Inverse Problems in Atmospheric Constituent Transport*, Cambridge University Press, Cambridge, UK, 2002.
- Evensen, G.: The ensemble Kalman filter: Theoretical formulation and practical implementation, *Ocean Dynam.*, 53, 343–367, 2003.

- Eyre, J.: A fast radiative transfer model for satellite sounding systems, ECMWF Research Dept. Tech. Memo, 176, 28 pp., 1991.
- Farquhar, G., von Caemmerer, S. V., and Berry, J.: A biochemical model of photosynthetic CO<sub>2</sub> assimilation in leaves of C3 species, *Planta*, 149, 78–90, 1980.
- Forget, G., Campin, J.-M., Heimbach, P., Hill, C. N., Ponte, R. M., and Wunsch, C.: ECCO version 4: an integrated framework for non-linear inverse modeling and global ocean state estimation, *Geosci. Model Dev.*, 8, 3071–3104, doi:10.5194/gmd-8-3071-2015, 2015.
- Giering, R. and Kaminski, T.: Recipes for Adjoint Code Construction, *ACM T. Math. Software*, 24, 437–474, doi:10.1145/293686.293695, 1998.
- Gobron, N., Pinty, B., Verstraete, M. M., and Govaerts, Y.: A semidiscrete model for the scattering of light by vegetation, *J. Geophys. Res.-Atmos.*, 102, 9431–9446, doi:10.1029/96JD04013, 1997.
- Govaerts, Y. M., Wagner, S., Lattanzio, A., and Watts, P.: Joint retrieval of surface reflectance and aerosol optical depth from MSG/SEVIRI observations with an optimal estimation approach: 1. Theory, *J. Geophys. Res.-Atmos.*, 115, d02203, doi:10.1029/2009JD011779, 2010.
- Griewank, A.: On Automatic Differentiation, in: *Mathematical Programming: Recent Developments and Applications*, edited by: Iri, M. and Tanabe, K., 83–108, Kluwer Academic Publishers, Dordrecht, 1989.
- Gómez-Dans, J. L., Lewis, P. E., and Disney, M.: Efficient Emulation of Radiative Transfer Codes Using Gaussian Processes and Application to Land Surface Parameter Inferences, *Remote Sens.*, 8, 119, doi:10.3390/rs8020119, 2016.
- Hascoët, L., Naumann, U., and Pascual, V.: “To Be Recorded” Analysis in Reverse-Mode Automatic Differentiation, *Future Generation Computer Systems*, 21, 1401–1417, doi:10.1016/j.future.2004.11.009, 2004.
- Heimann, M.: The Global Atmospheric Tracer Model TM2, Technical Report No. 10, Max-Planck-Institut für Meteorologie, Hamburg, Germany, 1995.
- Heimann, M. and Kaminski, T.: Inverse Modeling Approaches to Infer Surface Trace Gas Fluxes from Observed Atmospheric Mixing Ratios, in: *Approaches to scaling of trace gas fluxes in ecosystems*, edited by: Bouwman, A. F., Chap. 14, 275–295, Elsevier, Amsterdam, 1999.
- Heimann, M. and Körner, S.: The global atmospheric tracer model TM3, Tech. Rep. 5, Max-Planck-Institut für Biogeochemie, Jena, Germany, 2003.
- IPCC: Climate Change 2014: Synthesis Report. Contribution of Working Groups I, II and III to the Fifth Assessment Report of the Intergovernmental Panel on Climate Change, Core Writing Team, Pachauri, R. K. and Meyer, L. A. (Eds.), IPCC, Geneva, Switzerland, 151 pp., 2014.
- Isaksen, I., Bonavita, M., Buizza, R., Fisher, M., Haseler, J., Leutbecher, M., and Raynaud, L.: Ensemble of data assimilations at ECMWF, ECMWF, Reading, 2010.
- Jacquemoud, S. and Baret, F.: PROSPECT: A model of leaf optical properties spectra, *Remote Sens. Environ.*, 34, 75–91, doi:10.1016/0034-4257(90)90100-Z, 1990.
- Joiner, J. and Da Silva, A. M.: Efficient methods to assimilate remotely sensed data based on information content, *Q. J. Roy. Meteor. Soc.*, 124, 1669–1694, doi:10.1002/qj.49712454915, 1998.
- JungCLAUS, J. H., Lorenz, S. J., Timmreck, C., Reick, C. H., Brovkin, V., Six, K., Segschneider, J., Giorgetta, M. A., Crowley, T. J., Pongratz, J., Krivova, N. A., Vieira, L. E., Solanki, S. K., Klocke, D., Botzet, M., Esch, M., Gayler, V., Haak, H., Raddatz, T. J., Roeckner, E., Schnur, R., Widmann, H., Claussen, M., Stevens, B., and Marotzke, J.: Climate and carbon-cycle variability over the last millennium, *Clim. Past*, 6, 723–737, doi:10.5194/cp-6-723-2010, 2010.
- Kaminski, T. and Rayner, P. J.: Assimilation and Network Design, in: *Observing the continental scale Greenhouse Gas Balance of Europe*, edited by: Dolman, H., Freibauer, A., and Valentini, R., Ecological Studies, Chap. 3, 33–52, Springer-Verlag, New York, doi:10.1007/978-0-387-76570-9\_3, 2008.
- Kaminski, T. and Rayner, P. J.: Assisting the Evolution of the Observing System for the Carbon Cycle through Quantitative Network Design, *Biogeosciences Discuss.*, in press, 2017.
- Kaminski, T., Giering, R., Scholze, M., Rayner, P., and Knorr, W.: An example of an automatic differentiation-based modelling system, in: *Computational Science – ICCSA 2003, International Conference Montreal, Canada, May 2003, Proceedings, Part II*, edited by: Kumar, V., Gavrilova, L., Tan, C. J. K., and L’Ecuyer, P., Vol. 2668 of Lecture Notes in Computer Science, 95–104, Springer, Berlin, 2003.
- Kaminski, T., Scholze, M., and Houweling, S.: Quantifying the Benefit of A-SCOPE Data for Reducing Uncertainties in Terrestrial Carbon Fluxes in CCDAS, *Tellus B*, 62, 5, doi:10.1111/j.1600-0889.2010.00483.x, 2010.
- Kaminski, T., Knorr, W., Scholze, M., Gobron, N., Pinty, B., Giering, R., and Mathieu, P.-P.: Consistent assimilation of MERIS FAPAR and atmospheric CO<sub>2</sub> into a terrestrial vegetation model and interactive mission benefit analysis, *Biogeosciences*, 9, 3173–3184, doi:10.5194/bg-9-3173-2012, 2012a.
- Kaminski, T., Rayner, P. J., Voßbeck, M., Scholze, M., and Koffi, E.: Observing the continental-scale carbon balance: assessment of sampling complementarity and redundancy in a terrestrial assimilation system by means of quantitative network design, *Atmos. Chem. Phys.*, 12, 7867–7879, doi:10.5194/acp-12-7867-2012, 2012b.
- Kaminski, T., Knorr, W., Schürmann, G., Scholze, M., Rayner, P. J., Zaehle, S., Blessing, S., Dorigo, W., Gayler, V., Giering, R., Gobron, N., Grant, J. P., Heimann, M., Hooker-Stroud, A., Houweling, S., Kato, T., Kattge, J., Kelley, D., Kemp, S., Koffi, E. N., Köstler, C., Mathieu, P.-P., Pinty, B., Reick, C. H., Rödenbeck, C., Schnur, R., Scipal, K., Sebald, C., Stacke, T., van Scheltinga, A. T., Vossbeck, M., Widmann, H., and Ziehn, T.: The BETHY/JSBACH Carbon Cycle Data Assimilation System: experiences and challenges, *J. Geophys. Res.-Biogeo.*, 118, 1414–1426, doi:10.1002/jgrg.20118, 2013.
- Kaminski, T., Kauker, F., Eicken, H., and Karcher, M.: Exploring the utility of quantitative network design in evaluating Arctic sea ice thickness sampling strategies, *The Cryosphere*, 9, 1721–1733, doi:10.5194/tc-9-1721-2015, 2015.
- Kaminski, T., Pinty, B., Voßbeck, M., Lopatka, M., Gobron, N., and Robustelli, M.: Consistent EO Land Surface Products including Uncertainty Estimates, *Biogeosciences Discuss.*, doi:10.5194/bg-2016-310, in review, 2016a.
- Kaminski, T., Scholze, M., Knorr, W., Vossbeck, M., Buchwitz, M., and Reuter, M.: Constraining a terrestrial biosphere model with

- remotely sensed atmospheric carbon dioxide, *Remote Sens. Environ.*, under review, 2016b.
- Kauker, F., Kaminski, T., Ricker, R., Toudal-Pedersen, L., Dybkjaer, G., Melsheimer, C., Eastwood, S., Sumata, H., Karcher, M., and Gerdes, R.: Seasonal sea ice predictions for the Arctic based on assimilation of remotely sensed observations, *The Cryosphere Discuss.*, 9, 5521–5554, doi:10.5194/tcd-9-5521-2015, 2015.
- Kleespies, T., van Delst, P., McMillin, L., and Derber, J.: Atmospheric transmittance of an absorbing gas. 6. OPTRAN status report and introduction to the NESDIS/NCEP community radiative transfer model, *Appl. Optics*, 43, 3103–3109, 2004.
- Knorr, W., Kaminski, T., Scholze, M., Gobron, N., Pinty, B., Giering, R., and Mathieu, P.-P.: Carbon cycle data assimilation with a generic phenology model, *J. Geophys. Res.*, 115, G04017, doi:10.1029/2009JG001119, 2010.
- Lauvernet, C., Baret, F., Hascoët, L., Buis, S., and LeDimet, F.-X.: Multitemporal-patch ensemble inversion of coupled surface-atmosphere radiative transfer models for land surface characterization, *Remote Sens. Environ.*, 112, 851–861, 2008.
- Lauvernet, C., Hascoët, L., Le Dimet, F.-X., and Barret, F.: Using Automatic Differentiation to study the sensitivity of a crop model, in: *Recent Advances in Algorithmic Differentiation, Lecture Notes in Computational Science and Engineering*, 59–70, Springer, 2012.
- Lewis, P. E., Gomez-Dans, J., Kaminski, T., Settle, J., Quaife, T., Gobron, N., Styles, J., and Berger, M.: An Earth Observation Land Data Assimilation System (EO-LDAS), *Remote Sens. Environ.*, 120, 219–235, doi:10.1016/j.rse.2011.12.027, 2012.
- Lions, J. L.: *Optimal Control of Systems Governed by Partial Differential Equations*, Springer, Berlin/Heidelberg, 1971.
- Loew, A., van Bodegom, P. M., Widlowski, J.-L., Otto, J., Quaife, T., Pinty, B., and Raddatz, T.: Do we (need to) care about canopy radiation schemes in DGVMs? Caveats and potential impacts, *Biogeosciences*, 11, 1873–1897, doi:10.5194/bg-11-1873-2014, 2014.
- Lorenc, A. C. and Payne, T.: 4D-Var and the butterfly effect: Statistical four-dimensional data assimilation for a wide range of scales, *Q. J. Roy. Meteor. Soc.*, 133, 607–614, doi:10.1002/qj.36, 2007.
- Luo, Y. Q., Randerson, J. T., Abramowitz, G., Bacour, C., Blyth, E., Carvalhais, N., Ciais, P., Dalmonech, D., Fisher, J. B., Fisher, R., Friedlingstein, P., Hibbard, K., Hoffman, F., Huntzinger, D., Jones, C. D., Koven, C., Lawrence, D., Li, D. J., Mahecha, M., Niu, S. L., Norby, R., Piao, S. L., Qi, X., Peylin, P., Prentice, I. C., Riley, W., Reichstein, M., Schwalm, C., Wang, Y. P., Xia, J. Y., Zaehle, S., and Zhou, X. H.: A framework for benchmarking land models, *Biogeosciences*, 9, 3857–3874, doi:10.5194/bg-9-3857-2012, 2012.
- Marshall, J., Adcroft, A., Hill, C., Perelman, L., and Heisey, C.: A finite-volume, incompressible Navier Stokes model for studies of the ocean on parallel computers, *J. Geophys. Res.*, 102, 5753–5766, 1997.
- Masutani, M., Woollen, J. S., Lord, S. J., Emmitt, G. D., Kleespies, T. J., Wood, S. A., Greco, S., Sun, H., Terry, J., Kapoor, V., Treadon, R., and Campana, K. A.: Observing system simulation experiments at the National Centers for Environmental Prediction, *J. Geophys. Res.-Atmos.*, 115, D07101, doi:10.1029/2009JD012528, 2010.
- Mathieu, P. and O'Neill, A.: Data assimilation: From photon counts to Earth System forecasts, *Remote Sens. Environ.*, 112, 1258–1267, 2008.
- Melsheimer, C., Heygster, G., Mathew, N., and Pedersen, L.: Retrieval of Sea Ice Emissivity and Integrated Retrieval of Surface and Atmospheric Parameters over the Arctic from AMSR-E data, *J. Remote Sens. Soc. Jpn.*, 29, 236–241, 2009.
- Metropolis, N., Rosenbluth, A. W., Rosenbluth, M. N., Teller, A. H., and Teller, E.: Equation of state calculations for fast computing machines, *J. Chem. Phys.*, 21, 1087–1092, 1953.
- Migliorini, S.: On the Equivalence between Radiance and Retrieval Assimilation, *Mon. Weather Rev.*, 140, 258–265, doi:10.1175/MWR-D-10-05047.1, 2012.
- Moncet, J.-L., Uymin, G., Lipton, A. E., and Snell, H. E.: Infrared Radiance Modeling by Optimal Spectral Sampling, *J. Atmos. Sci.*, 65, 3917–3934, doi:10.1175/2008JAS2711.1, 2008.
- Moore, A., Arango, H., Di Lorenzo, E., Cornuelle, B., Miller, A., and Neilson, D.: A comprehensive ocean prediction and analysis system based on the tangent linear and adjoint of a regional ocean model, *Ocean Model.*, 7, 227–258, doi:10.1016/j.ocemod.2003.11.001, 2004.
- O'Dell, C. W., Heidinger, A. K., Greenwald, T., Bauer, P., and Ben-nartz, R.: The successive-order-of-interaction radiative transfer model. Part II: Model performance and applications, *J. Appl. Meteorol. Clim.*, 45, 1403–1413, 2006.
- Pascual, V. and Hascoët, L.: TAPENADE for C, in: *Advances in Automatic Differentiation, Lecture Notes in Computational Science and Engineering*, 199–210, Springer, selected papers from AD2008 Bonn, August 2008.
- Pinty, B., Gobron, N., Widlowski, J., Gerstl, S., Verstraete, M., Antunes, M., Bacour, C., Gascon, F., Gastellu, J., Goel, N., Jacquemoud, S., North, P., Qin, W., and Thompson, R.: Radiation transfer model intercomparison (RAMI) exercise, *J. Geophys. Res.*, 106, 11937–11956, 2001.
- Pinty, B., Lavergne, T., Dickinson, R., Widlowski, J., Gobron, N., and Verstraete, M.: Simplifying the interaction of land surfaces with radiation for relating remote sensing products to climate models, *J. Geophys. Res.*, 111, 2156–2202, doi:10.1029/2005JD005952, 2006.
- Pinty, B., Lavergne, T., Voßbeck, M., Kaminski, T., Aussedat, O., Giering, R., Gobron, N., Taberner, M., Verstraete, M. M., and Widlowski, J.-L.: Retrieving surface parameters for climate models from MODIS-MISR albedo products, *J. Geophys. Res.*, 112, D10116, doi:10.1029/2006JD008105, 2007.
- Pinty, B., Andredakis, I., Clerici, M., Kaminski, T., Taberner, M., Verstraete, M. M., Gobron, N., Plummer, S., and Widlowski, J.-L.: Exploiting the MODIS albedos with the Two-stream Inversion Package (JRC-TIP): 1. Effective leaf area index, vegetation, and soil properties, *J. Geophys. Res.-Atmos.*, 116, D09105, doi:10.1029/2010JD015372, 2011a.
- Pinty, B., Clerici, M., Andredakis, I., Kaminski, T., Taberner, M., Verstraete, M. M., Gobron, N., Plummer, S., and Widlowski, J.-L.: Exploiting the MODIS albedos with the Two-stream Inversion Package (JRC-TIP): 2. Fractions of transmitted and absorbed fluxes in the vegetation and soil layers, *J. Geophys. Res.-Atmos.*, 116, D09106, doi:10.1029/2010JD015373, 2011b.
- Rabier, F., Jarvinen, H., Klinker, E., Mahfouf, J.-F., and Simmons, A.: The ECMWF operational implementation of four-dimensional variational assimilation. Part I: Experimental results

- with simplified physics, *Q. J. Roy. Meteor. Soc.*, 126, 1143–1170, 2000.
- Rahman, H. and Dedieu, G.: SMAC: a simplified method for the atmospheric correction of satellite measurements in the solar spectrum, *Int. J. Remote Sens.*, 15, 123–143, doi:10.1080/01431169408954055, 1994.
- Rayner, P., Scholze, M., Knorr, W., Kaminski, T., Giering, R., and Widmann, H.: Two decades of terrestrial Carbon fluxes from a Carbon Cycle Data Assimilation System (CCDAS), *Global Biogeochem. Cy.*, 19, GB2026, doi:10.1029/2004GB002254, 2005.
- Rayner, P. J. and O'Brien, D. M.: The utility of remotely sensed CO<sub>2</sub> concentration data in surface source inversions, *Geophys. Res. Lett.*, 28, 175–178, 2001.
- Reuter, M., Bovensmann, H., Buchwitz, M., Burrows, J. P., Connor, B. J., Deutscher, N. M., Griffith, D. W. T., Heymann, J., Keppel-Aleks, G., Messerschmidt, J., Notholt, J., Petri, C., Robinson, J., Schneising, O., Sherlock, V., Velazco, V., Warneke, T., Wennberg, P. O., and Wunch, D.: Retrieval of atmospheric CO<sub>2</sub> with enhanced accuracy and precision from SCIAMACHY: Validation with FTS measurements and comparison with model results, *J. Geophys. Res.*, 116, D04301, doi:10.1029/2010JD015047, 2011.
- Reuter, M., Hilker, M., Schneising, O., Buchwitz, M., and Heymann, J.: ESA Climate Change Initiative (CCI) Comprehensive Error Characterisation Report: BESD full-physics retrieval algorithm for XCO<sub>2</sub> for the Essential Climate Variable (ECV) Greenhouse Gases (GHG) Version 2.0, revision 1, Tech. rep., available at: [http://www.esa-ghg-cci.org/webfm\\_send/284](http://www.esa-ghg-cci.org/webfm_send/284) (last access: 4 May 2017), 2016.
- Rodgers, C. D. and Connor, B. J.: Intercomparison of remote sounding instruments, *J. Geophys. Res.-Atmos.*, 108, 4116, doi:10.1029/2002JD002299, 2003.
- Saunders, R., Matricardi, M., and Brunel, P.: An improved fast radiative transfer model for assimilation of satellite radiance observations, *Q. J. Roy. Meteor. Soc.*, 125, 1407–1425, 1999.
- Scholze, M., Kaminski, T., Knorr, W., Blessing, S., Vossbeck, M., Grant, J., and Scipal, K.: Simultaneous assimilation of {SMOS} soil moisture and atmospheric {CO<sub>2</sub>} in-situ observations to constrain the global terrestrial carbon cycle, *Remote Sens. Environ.*, 180, 334–345, doi:10.1016/j.rse.2016.02.058, 2016.
- Schürmann, G. J., Kaminski, T., Köstler, C., Carvalhais, N., Voßbeck, M., Kattge, J., Giering, R., Rödenbeck, C., Heimann, M., and Zaehle, S.: Constraining a land-surface model with multiple observations by application of the MPI-Carbon Cycle Data Assimilation System V1.0, *Geosci. Model Dev.*, 9, 2999–3026, doi:10.5194/gmd-9-2999-2016, 2016.
- Smith, D. M., Scaife, A. A., Boer, G. J., Caiian, M., Doblas-Reyes, F. J., Guemas, V., Hawkins, E., Hazeleger, W., Hermanson, L., Ho, C. K., Ishii, M., Kharin, V., Kimoto, M., Kirtman, B., Lean, J., Matei, D., Merryfield, W. J., Müller, W. A., Pohlmann, H., Rosati, A., Wouters, B., and Wyser, K.: Real-time multi-model decadal climate predictions, *Clim. Dynam.*, 41, 2875–2888, doi:10.1007/s00382-012-1600-0, 2013.
- Snyder, C., Bengtsson, T., Bickel, P., and Anderson, J.: Obstacles to High-Dimensional Particle Filtering, *Mon. Weather Rev.*, 136, 4629–4640, doi:10.1175/2008MWR2529.1, 2008.
- Stammer, D., Wunsch, C., Giering, R., Eckert, C., Heimbach, P., Marotzke, J., Adcroft, A., Hill, C. N., and Marshall, J.: The global ocean circulation during 1992–1997, estimated from ocean observations and a general circulation model, *J. Geophys. Res.*, 107, 3118, doi:10.1029/2001JC000888, 2002.
- Stockdale, T., Anderson, D., Balmaseda, M., Doblas-Reyes, F., Ferranti, L., Mogensen, K., Palmer, T., Molteni, F., and Vitart, F.: ECMWF seasonal forecast system 3 and its prediction of sea surface temperature, *Clim. Dynam.*, 37, 455–471, doi:10.1007/s00382-010-0947-3, 2011.
- Talagrand, O.: The Use of Adjoint Equations in Numerical Modelling of the Atmospheric Circulation, in: *Automatic Differentiation of Algorithms: Theory, Implementation, and Application*, edited by: Griewank, A. and Corliss, G. F., 169–180, SIAM, Philadelphia, Penn., 1991.
- Tarantola, A.: *Inverse Problem Theory and methods for model parameter estimation*, SIAM, Philadelphia, 2005.
- Timmermans, R., Lahoz, W., Attié, J.-L., Peuch, V.-H., Curier, R., Edwards, D., Eskes, H., and Builtjes, P.: Observing System Simulation Experiments for air quality, *Atmos. Environ.*, 115, 199–213, doi:10.1016/j.atmosenv.2015.05.032, 2015.
- Tonboe, R., Andersen, S., Toudal, L., and Heygster, G.: Sea ice emission modelling, in: *Thermal Microwave Radiation – Applications for Remote Sensing*, edited by: Mätzler, C., Rosenkranz, P. W., Battaglia, A., and Wigneron, J. P., IET Electromagnetic Waves Series 52, London, UK, 2006.
- Toudal, L.: Merging microwave radiometer data and meteorological data for improved sea ice concentrations, *EARSeL Advances in Remote Sensing*, 3, 81–89, 1994.
- van Leeuwen, P. J.: Particle Filtering in Geophysical Systems, *Mon. Weather Rev.*, 137, 4089–4114, doi:10.1175/2009MWR2835.1, 2009.
- Verhoef, W.: Light scattering by leaf layers with application to canopy reflectance modeling: The SAIL model, *Remote Sens. Environ.*, 16, 125–141, doi:10.1016/0034-4257(84)90057-9, 1984.
- Vermote, E., Tanré, D., Deuze, J., Herman, M., and Morcette, J.: Second simulation of the satellite signal in the solar spectrum, 6S: An overview, *IEEE T. Geosci. Remote Sens.*, 35, 675–686, 1997.
- Weaver, A., Vialard, J., and Anderson, D.: Three- and four-dimensional variational assimilation with a general circulation model of the tropical Pacific Ocean. Part I: Formulation, internal diagnostics, and consistency checks, *Mon. Weather Rev.*, 131, 1360–1378, 2003.
- Widlowski, J.-L., Taberner, M., Pinty, B., Bruniquel-Pinel, V., Disney, M., Fernandes, R., Gastellu-Etchegorry, J.-P., Gobron, N., Kuusk, A., Lavergne, T., Leblanc, S., Lewis, P. E., Martin, E., Möttus, M., North, P. R. J., Qin, W., Robustelli, M., Rochdi, N., Ruiloba, R., Soler, C., Thompson, R., Verhoef, W., Verstraete, M. M., and Xie, D.: Third Radiation Transfer Model Intercomparison (RAMI) exercise: Documenting progress in canopy reflectance models, *J. Geophys. Res.-Atmos.*, 112, d09111, doi:10.1029/2006JD007821, 2007.
- Widlowski, J.-L., Pinty, B., Lopatka, M., Atzberger, C., Buzica, D., Chelle, M., Disney, M., Gastellu-Etchegorry, J. P., Gerboles, M., Gobron, N., Grau, E., Huang, H., Kallel, A., Kobayashi, H., Lewis, P., Qin, W., Schlerf, M., Stuckens, J., and Xie, D.: The fourth radiation transfer model intercomparison (RAMI-IV): Proficiency testing of canopy reflectance models with ISO-13528, *J. Geophys. Res.-Atmos.*, 118, 6869–6890, doi:10.1002/jgrd.50497, 2013.

- Widlowski, J.-L., Mio, C., Disney, M., Adams, J., Andreadakis, I., Atzberger, C., Brennan, J., Busetto, L., Chelle, M., Ceccherini, G., Colombo, R., Côté, J.-F., Eenmäe, A., Essery, R., Gastellu-Etchegorry, J. P., Gobron, N., Grau, E., Haverd, V., Homolová, L., Huang, H., Hunt, L., Kobayashi, H., Koetz, B., Kuusk, A., Kuusk, J., Lang, M., Lewis, P., Lovell, J. L., Malenovsky, Z., Meroni, M., Morsdorf, F., Möttus, M., Ni-Meister, W., Pinty, B., Rautiainen, M., Schlerf, M., Somers, B., Stuckens, J., Verstraete, M. M., Yang, W., Zhao, F., and Zenone, T.: The fourth phase of the radiative transfer model intercomparison (RAMI) exercise: Actual canopy scenarios and conformity testing, *Remote Sens. Environ.*, 169, 418–437, doi:10.1016/j.rse.2015.08.016, 2015.
- Wiesmann, A. and Mätzler, C.: Microwave emission model of layered snowpacks, *Remote Sens. Environ.*, 70, 307–316, 1999.
- Wunsch, C. and Heimbach, P.: Estimated Decadal Changes in the North Atlantic Meridional Overturning Circulation and Heat Flux 1993–2004, *J. Phys. Oceanogr.*, 36, 2012–2024, doi:10.1175/JPO2957.1, 2006.
- Wunsch, C., Heimbach, P., Ponte, R., and Fukumori, I.: The global general circulation of the ocean estimated by the ECCO-Consortium, *Oceanography*, 22, 88–103, 2009.
- Xu, Q.: Generalized Adjoint for Physical Processes with Parameterized Discontinuities. Part I: Basic Issues and Heuristic Examples, *J. Atmos. Sci.*, 53, 1123–1142, doi:10.1175/1520-0469(1996)053<1123:GAFPPW>2.0.CO;2, 1996.
- Zupanski, D.: A general weak constraint applicable to operational 4DVAR data assimilation systems, *Mon. Weather Rev.*, 125, 2274–2292, 1997.